AUT Journal of Civil Engineering

AUT J. Civil Eng., 4(1) (2020) 3-16
DOI: 10.22060/ajce.2019.15680.5547

Effects of mechanical coupler on cyclic behavior of wet connection in precast concrete Frame

E. Mobedi[1], H. Parastesh[1] and A. Khaloo[2]

[1]Department of Civil Engineering, University of Science and Culture, Tehran, Iran
[2]Department of Civil Engineering, Sharif University of Technology, Tehran, Iran

ABSTRACT: Too many efforts have been made to study the structural behavior of precast concrete moment-resisting connections subjected to seismic excitations. Mechanical reinforcement couplers (MRCs) are one of the main solutions for enhancing the ductility and energy absorption in the precast connection zone. The main novelty of this research is to propose an efficient precast connection using MRCs and grout. The current paper is attempted to explore the effects of the MRCs on the precast concrete connection cyclic load protocols. MRC connection is comprised of an innovative detailing for joining the reinforcement bars using couplers and the cast-in-place concrete was used to construct the connection zone. Several test specimens with various couplers array were prepared to a comprehensive survey on the seismic behavior of the connection zone. The displacement control procedure of the test program was simulated in the ABAQUS software. The numerical and experimental results are analyzed to evaluate the moment carrying capacity, energy dissipation, and ductility variations. The differences of failure modes of the monolithic and new precast connection were investigated by detection of the crack propagation procedure through the test monitoring and simulation visualization. The test results of the MRC-equipped specimens were compared with those of numerical models. Both numerical simulation and test program leads to same results which demonstrated that the moment carrying capacity and energy dissipation are significantly improved. The crack propagation pattern in the monolithic sample was different from the precast specimens.

Review History:
Received: 2019-01-21
Revised: 2019-04-20
Accepted: 2019-04-23
Available Online: 2019-04-23

Keywords:
Precast concrete
Mechanical Splice Coupler
Semi-dry connection
Cast in Place Concrete
Seismic behavior

1. INTRODUCTION

As the modern world aspect is the higher quality of life accompanying with new definition of safety and life style, the known construction companies establish new precast construction method to improve the quality and construction speed. One the main modern construction methods are precast concrete modular approach. As the critical issue in the precast method is the connection zone behavior in the seismically high-risk regions, researchers focused on providing innovative details for promoting the connection zone behavior.

The main results of these investigations are presented in the design codes such as PRESSS (Precast Seismic Structural System Research Program), which is a US-Japan joint research program for precast concrete building systems suitable for seismic conditions, the American ACI 550 1R-09 Code, New Zealand's "Guidelines for the Use of Standard Structural Precast Concrete in Buildings," and Japan's JASS10 Code [1-4].

Vidjeapriya and Jaya studied the effect of J-Bolts and cleat angles on the hysteretic behavior of precast beam–column connections. They found that using J-Bolts for the beam–column connection leads to higher ductility as well as energy dissipation in comparison to similar monolithic specimens, while using cleat angles for the connections leads to less ductility [5].

Daisuke proposed a wet connection comprised of sleeve splices for bending reinforcement. Three types of precast concrete beam-column connections were compared with a cast-in-place one. The study results demonstrated that the proposed precast connection provides lower initial stiffness and shear strength in relation to monolithic connection [6].

Ozden et al. investigated five different types of precast concrete frame connections, including one cast-in-place connection, two precast wet connections (at the end of the beam and column) and two precast dry connections (welded and bolted with brackets). According to their results, the bolted connection showed the maximum strength, ductility and energy dissipation rates [7].

Parastesh et al. investigated a new ductile moment-resisting beam-column connection for precast reinforced concrete frames in high seismic zones including lap splice rebar. Their proposed connection provided higher structural integrity, flexural strength, drift capacity, ductility and energy dissipation compared to similar cast-in-place specimens [8]. Wu et al. conducted experiments on a precast concrete connection in comparison to a cast-in-place connection.

*Corresponding author's email: parastesh@usc.ac.ir

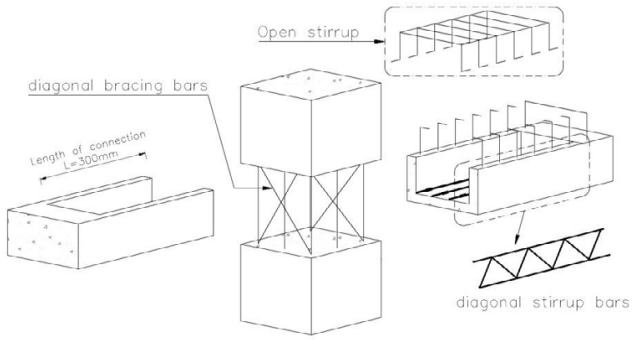

Fig. 1. The connection zone reinforcing details for different coupler arrangement

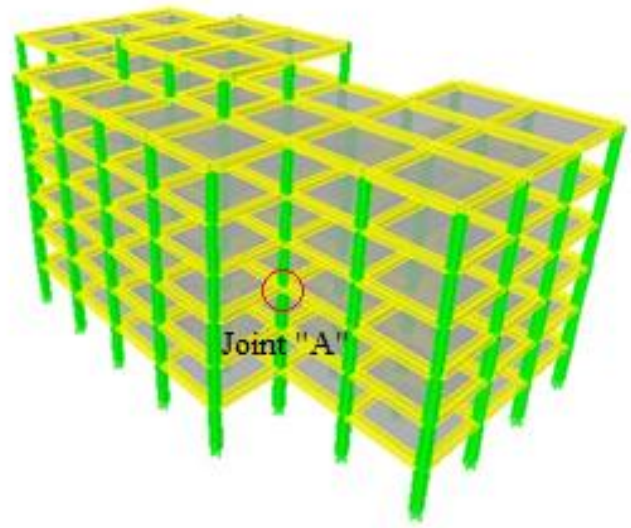

Fig. 2. Precast connection prototype design, Target building

Their study results demonstrated a similar hysteretic behavior for the connections; however, the degradation velocity of the bearing capacity of the precast connection was higher than that of the cast-in-place connection. [9].

Some studies have also taken the use of MRCs in the precast concrete connections into account. Bai et al. investigated the seismic performance verification of a spiral thread mechanical reinforcement connection system to be used in reinforced concrete structures. Both in-air component tests and structural subassembly tests have been conducted to evaluate the connection efficiency [10]. They used two external beam–column connection subassemblies with spiral thread mechanical reinforcement couplers installed at the column–joint interface. The connections were subjected to simulated seismic cyclic loads. Their study results proved that uniaxial tensile tests are unable to accurately demonstrate probable coupler performance in plastic hinge zones.

Haber et al. studied five half-scale bridge column models subjected to reverse slow cyclic loading [11]. Their study aimed to develop four new moment connections at column-footing joints for reducing bridge construction time in high seismic regions. Mechanical splices (an upset headed coupler and a grout-filled sleeve coupler) were used in the new connections in precast columns to be connected to bars in a cast-in-place footing. They found that the seismic performance of the new connections was similar to that of conventional cast-in-place specimens. Bompa and Elghazouli investigated more than 350 specimens extracted from the literature to determine their performance in terms of geometry, ductility, and strength [12]. Based on the results of their study, PTC (parallel thread coupler) provides the most efficient connection from the structural and constructional point of view.

Bahrami et al. invented a precast connection consist of a continuous column and two corbels connected to beams. These corbels were connected to the connection parts provided below the beams using screws or welding. Results of the parametric studies on the proposed connection demonstrate that the connection response includes the strength, ductility, rigidity, and energy dissipation can reach approximately 80% of the monolithic constructed connections [13].

Fathi et al. invented a type of metal connection consist of welded metal plates and gussets in order to connect the precast continuous concrete column to the semi-precast concrete beams. This connection was connected to the beam using screws or welding. Based on the numerical and experimental results, this connection shows a performance similar to that of the monolithic constructed connection [14].

A new precast connection detail with MRCs is introduced in the current study. The seismic behavior of the proposed connection is investigated through a comprehensive numerical and experimental search program. The test assembly was set up to apply a constant axial load accompanying with a lateral cyclic load. The numerical models were prepared elaborately based on the details of the test specimens. The study results are interpreted to investigate the efficiency of the proposed connection. The results prove the key role of the MRCs in the heightening of the energy absorption and ductility of the connection zone.

2- RESEARCH SIGNIFICANCE

The mechanical reinforcement couplers (MRCs) are one of the prevalent methods for joining the bars. The novelty of the current research is to implement the MRCs in a semi-dry precast connection. The application of MRCs decreases the rebar congestion in the connection zone of precast frame structures. Ease of assembly and increasing the construction speed are of the leading advantages of the proposed connection. The MRCs coupler arrangement can affect the Flexural capacity, energy dissipation, failure modes, and moment curvature of prefabricated specimens.

3-TEST PROGRAM

3-1-Connection details

The schematic details of the moment-resisting precast connection are shown in the Fig.. 1. The concrete part of the precast column was removed in the vicinity of the connection zone to provide the precast beam installation space. The strength and rigidity of the column was protected by four diagonal bars during the installation process. These diagonal bars are implemented in the column connection area. As illustrated in Fig.. 1, the diagonal transversal stirrups were

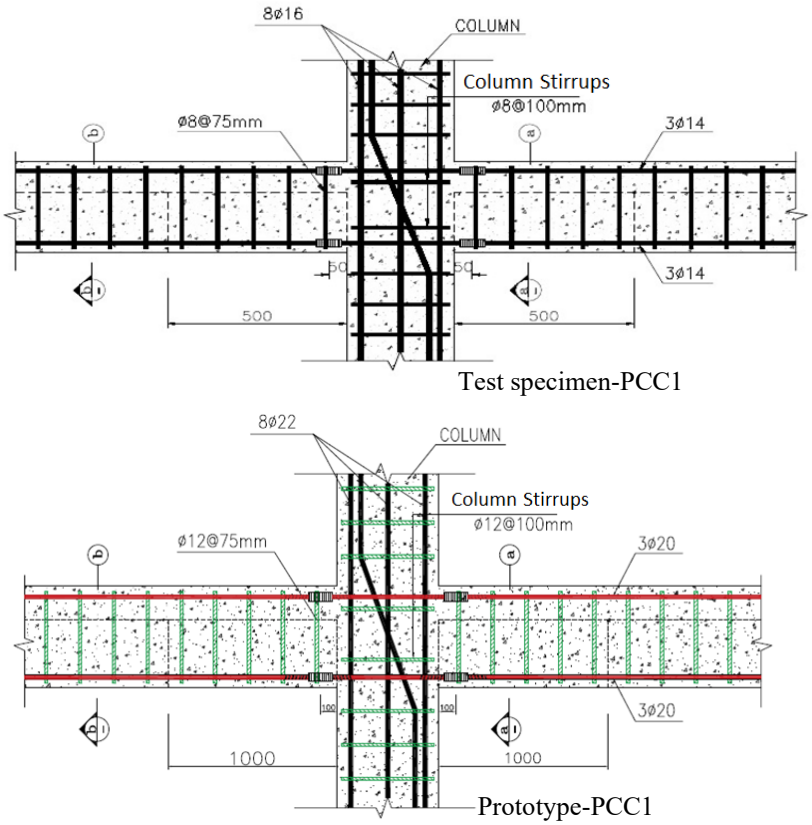

Fig. 3. Prototype and test specimen details

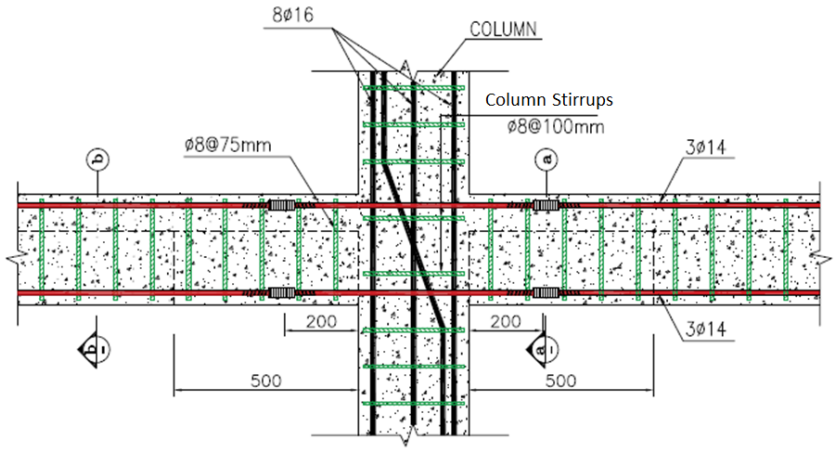

Fig. 4. The test specimen details (PCF1)

placed in U shaped cross-section beams to provide enough shear strength against set up loading. In order to assure the integrity of precast members, cast in place concrete was used in the connection zone. So one third of the beam section height is grouted in the vicinity of the connection zone.

3-2-Basic design of the test specimens

A four-story administrative building was considered to design the prototype of the test specimens. The precast concrete building included plan dimensions of 24m × 30m, 6m column spacing and 3.4m story height (See Fig.. 2). The test specimens were made to half scaled of joint "A" as interior beam-to-column joint of the building. The two directional moment-resisting frames were considered as lateral resisting system for this building. The column dimensions were 600 ×600mm. The gravity and seismic loading are determined based on IBC 2016 and ASCE-7-2010, respectively [15-16]. The test specimen details were prepared exactly according to the seismic provision of the ASCE-7-2010 for zone 4 and soil type D. A moderate ductility is assumed by ductility factor (Rw) of 8. The beams in the prototype were 600×600mm and carried a factored moment (Mu) of 240 KN-m at the column face. The design compressive strength of concrete columns and beams was 25 MPa and the yield strength of

Fig.5 Tensile test specimen

Table 1. Test specimens properties

Model name	Normal concrete MPa	Grout MPa	Notes
MC1	25	-	Beam and column are cast in-place (monolithic constructed specimen)
PCF1	25	25	Connection zone is grouted, and the location of the couplers is 20 cm from the column face.
PCC1	25	25	Connection zone is grouted, and the location of the couplers is 5 cm from the column face.

reinforcements for longitudinal and transverse bars was 400 MPa and 300 MPa respectively. The same concrete and steel material properties were considered for prototype and test specimen. The structural members were designed according to ACI-318-2017 [17]. Fig. 3 was illustrated the test specimens and prototype details.

3-3-Test specimen details

Fig. 4 provides the details of the half scale test specimens with a factor of S=0.5 for length and (S)2 factor for cross-sectional area of reinforcements. In addition to monolithic specimen, two half-scaled precast specimens were constructed to study the connection behavior. The direct tensile test was carried out for typical bars connected with the couplers to ensure the quality of them. Fig. .5 displays the failure mode of the tensile test specimen so that the rupture was occurred outside of the coupler zone and proved the adequate strength of the coupler material. The geometric properties of the test specimens are summarized in the Table 1.

The columns were continuously cast with the exception of the joint zone. Diagonal bars were used in the joint region of the column element to provide sufficient stability during the column installation in the lab.

The connection region was grouted after placing the longitudinal reinforcement bars. The specimens were then centered between two rigid steel frame columns that were fixed to the strong floor of the lab. Fig.. 6 shows the schematic view of connections state. Roller supports were used at the ends of the beam and top of the column and a hinge support was used at the column base as shown in Fig.. 6.

Half depth of the beam was prefabricated and the upper half of beam was completed with cast in place concrete in the lab to develop a perfect integrity between column and beam. To provide sufficient splice development length at the connection zones, the U shaped stirrups was considered at the top of precast part of the beam to ensure the shear strength of the section under lateral loading. The connection region will be grouted to form a monolithic connection. The precast beam and column are connected either by mechanical splices in preformed ducts which with subsequently filled by grout injection.

The couplers were placed in the different distances from the precast column face to experience two different plastic hinge scenarios. PCC1 and PCF1 are respectively referred to the specimens with the 50 mm and the 200 mm distances from the column face.

As the couplers has higher yield strength in relation to the flexural bars, the flexural strength increases at the vicinity of the connection zone. Also, the reinforcement congestion is reduced by using the couplers which in-turn increase the concrete quality at the connection zone. Closer stirrups were used to achieve complete bending rigidity by providing more confinement for the concrete parts in the connection zone. The skewed bars were implemented in the columns at the connection zone to ensure the shear strength of the connection zone.

4- TEST SET-UP

The interior connection is assembled with column height of 1700 mm and the beam length of 1500 mm. The couplers facilitate the assembly of the longitudinal bars. The steel reaction wall accompanied with a strong floor was utilized to fix the specimen as shown in Fig..6. The rollers supported were used at the ends of the beam. Also, the specimens were pinned at the base of column. Two actuators were used to product lateral movement.

As illustrated in Fig.. 6, three load cells were installed at the top of the column to record the exerted lateral and vertical loads. Fig..6 displays LVDTs position for measurement of the specimen displacements. The LVDTs properties are presented in Table 2. The strain gauge labels are illustrated in Fig..7.

Some strain gauges were used to measure the strains of steel rebars, control bond slip behavior and the yield lateral displacement of the joints. 24 strain gauges were installed on the beam reinforcement bars behind the couplers to monitor maximum strain and stress in steel reinforcement; also, 16 strain gauges were applied in longitudinal column bars so demonstrated in Fig..7.

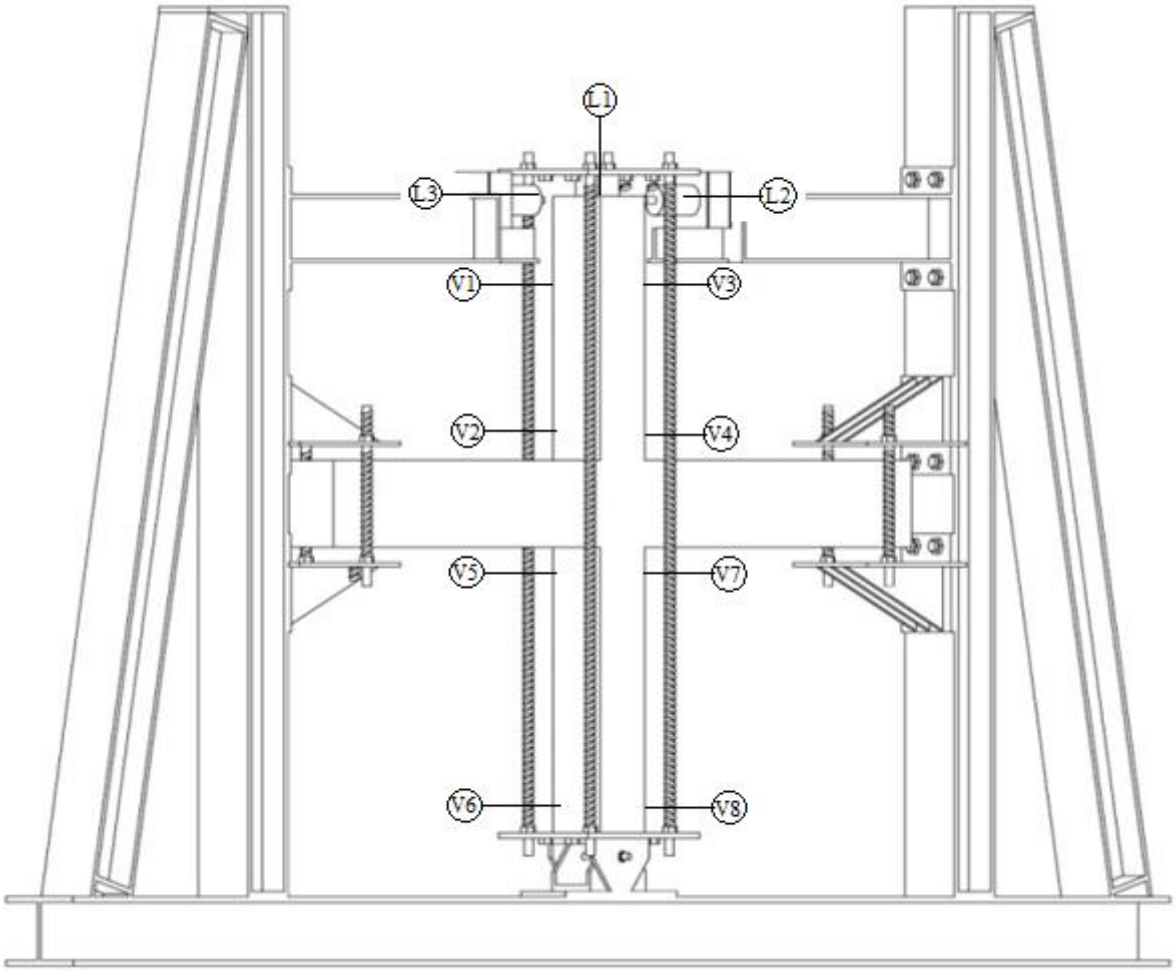

Fig. 6 The test set-up (L-load cell; V-LVDT)

Table. 2. LVDTs properties

Categories	Performance index
Gate resistance	120.0 ± 0.3 Ω
Gate factor	2.14 ± 2%
Precision grade	A
Fence long	3 × 2mm

4-1-Test method

An axial load equal to 0.1 f_c' Ag was applied on the top of column by prestressing the column. This is approximately half of the axial load experienced by an interior column in the first story of the prototype structure. The cyclic lateral load was load control for the first cycles up to yielding displacement and afterward the load control cycles were transformed to displacement control ones. The lateral load was exerted at the top of column (See Fig.. 6). The yield displacement, Δ_y , was defined as the 4/3 times of the displacement corresponding to the 0.75 of the calculated ultimate moment at the connection. The maximum displacement applied (see Fig.. 8) was ± 10 Δ_y . The failure criterion was selected based on 80 percent of the maximum applied lateral load. The actuators were stopped at every half cycle to facilitate the detection of the cracks propagations. The ultimate lateral displacement of a 102 mm (6% lateral drift) was considered to stop the loading. A TML static data logger (shown in Fig.. 9) with 32 channels is implemented to acquire the test results at a sampling frequency of 1 Hz.

5-NUMERICAL MODELS FEATURES

The numerical models dimensioned based on the test specimen of the precast middle joint with actual scale. The details of cast-in-place and precast models for middle joints are shown in Fig.. 4. The precast connection was designed by assuming the behavior of the monolithic constructed connection. Fig.. 10 presents a 3D model of the PCF-1

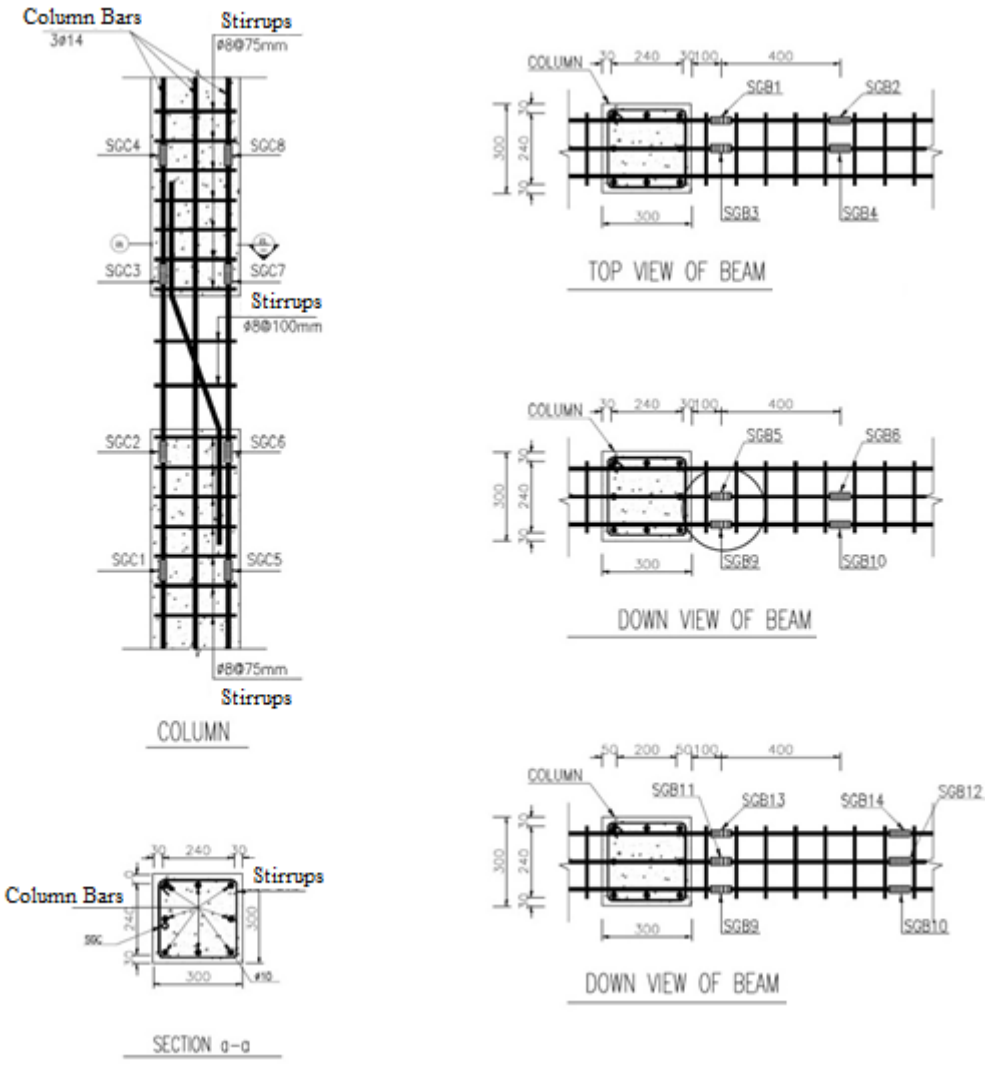

Fig. 7.Strain gauge installation format for reinforcement (dimension in mm)

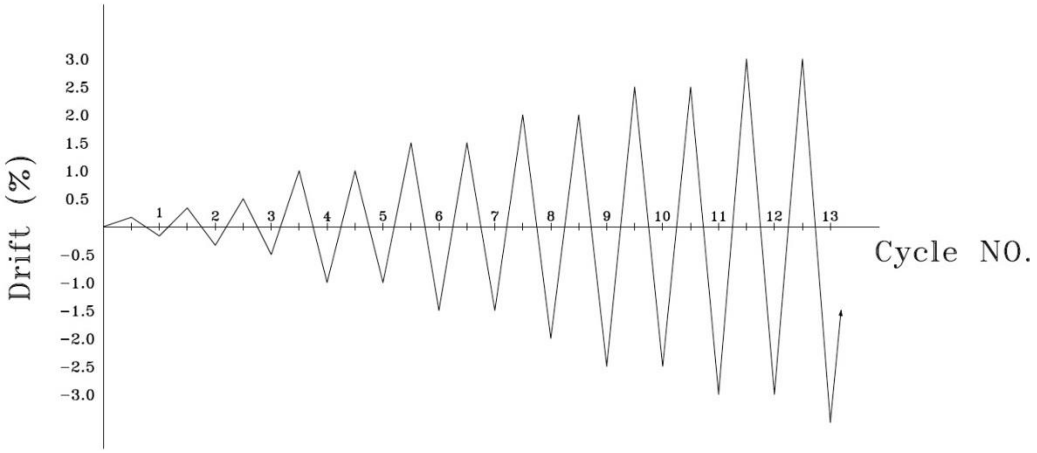

Fig. 8. Lateral cyclic loading protocol [8]

specimen whose features are presented in Table 1.

All specimens were tested under constant axial load (10% the axial load-bearing capacity of the column) and lateral cyclic loading on the column. Fig.. 11 presents the loading, boundary conditions, and length of beam and column members in the middle joints. The lateral load was applied based on the Fig.. 8 exactly the same as the test program.

A summary of the features of models used in this study

Fig. 9. Data acquisition apparatus (TML)

is given in Table 1. The MC1 model is the observant one (monolithic model with no couplers). PCC1 and PCF1 models were classified in terms of the array of couplers as described in the details of the test specimens.

5-1- Finite Element method

For the 3D modeling and non-linear analysis of the reinforced concrete connections, the ABAQUS software was utilized. The conventional elastoplastic model was considered to define the behavior of steel. The modulus elasticity, the Poisson's coefficient and the yield stress of the steel bar material were assumed to be 204000 MPa, 0.3 and 400 MPa, respectively. The mechanical properties of concrete were determined based on concrete test features. The density, the elasticity module and Poisson's coefficient of the concrete material was considered to be 2400 kg/m3, 23400 MPa and 0.2, respectively. The concrete damage plasticity (CDP) model was applied to consider a non-linear behavior for the concrete [18]. This model is appropriate for concrete under dynamic or cyclic loading as well as static loading. In this model, two major failure mechanisms of concrete, i.e. tensile cracking and compressive crushing, were considered. The compressive behavior of concrete is modified to consider the confinement effects of transvers reinforcement steels based on the procedure proposed by Mander [19] (Fig.. 12 and 13). The CDP constitutive material law considers the tensile behavior of the concrete after tensile failure. The tensile strength of concrete is assumed to be 10 percent of the concrete's uniaxial compressive strength, i.e. 2.5 MPa. The post-failure strain is considered for a strain ranges about ten times of the ultimate elastic strain. The effects of interactions between concrete and reinforcement steel are considered by defining the post-failure behavior of concrete. Therefore, the bond-slip effects are considered between reinforcement steel and concrete, such that, after the tensile failure of the concrete parts, the load is transferred from cracks to reinforcement steels [18].

The potential function used for the plastic behavior of the concrete is the Drucker-Prager hyperbolic equation. Also, the Lubliner yield surface with modifications proposed by Lee and Fenves are considered for definition of the constitutive material law [18,20].

The dynamic explicit non-linear method was employed for analysis of the connection. The selected method applies the central-difference rule for solving non-linear equations. In contrast to implicit solution method, the explicit methods do not require estimating the response in the next step time ($t+\Delta t$), therefore there is no need to trial and error process and also convergence tolerance. The mass-scaling parameter was set to be one and the extremums of the results were compared to achieve fair agreement. Fig.. 11 displays loading type and boundary conditions. The eight-node reduced integrated cubic elements C3D8R were selected for the concrete parts. The dual-node 3D truss element T3D2 was utilized for reinforcement bars and couplers. The reinforcement element nodes were constrained to the closest nodes of the C3D8R elements of the concrete parts by means of the "Embedded elements" technique [18]. The preferred mesh size of the elements was assumed to be 30 mm for concrete and bar elements. The mesh dimensions were calibrated based on the test results. Plasticity parameters of the CDP model are presented in the table. 3. These parameters were utilized in the CDP model for formation of the yield surface.

6- RESULTS AND DISCUSSION

The numerical and experimental results are analyzed to achieve the failure modes, drift capacity, flexural strength, strength degradation, ductility, and energy dissipation and connection stiffness. The hysteresis curves of the load-displacement are presented in the Fig..14. The envelop curves are also provided on each cyclic load-displacement results. The power of the simulation method can be discussed based on the Fig.. 14. As it can inferred from the Fig.. 14 the ultimate results are so close to each other and shows a 3.5 percent deviation. The extreme bounds of the curves in the experimental and numerical curves have been considered to compare the results in the Fig.. 14. The other verification criteria are under the curve area of the envelopes. As the CDP material model is not applicable for simulation of the pinching effect, the deviation of the results in the later criteria are slightly more than before mentioned ones. This issue also can be observed in the numerical results presented by Ab-Kadir et al. [22]. The deviation for under the envelope cure area is determined about 8.1 %.

6-1-Failure modes

The typical crack propagation of the test specimens were illustrated in Fig..15. Generally, the specimen experiences the different states during the cyclic loading: Crack initiation and development, yield state, ultimate bearing capacity and eventually the failure mode. The crack propagation caused by interactions of the axial force, bending moment, and shear force that lead to a very complicated stress state in the connection zone.

At the first step of loading, the flexural cracks can be observed on the intersection of beam to column while

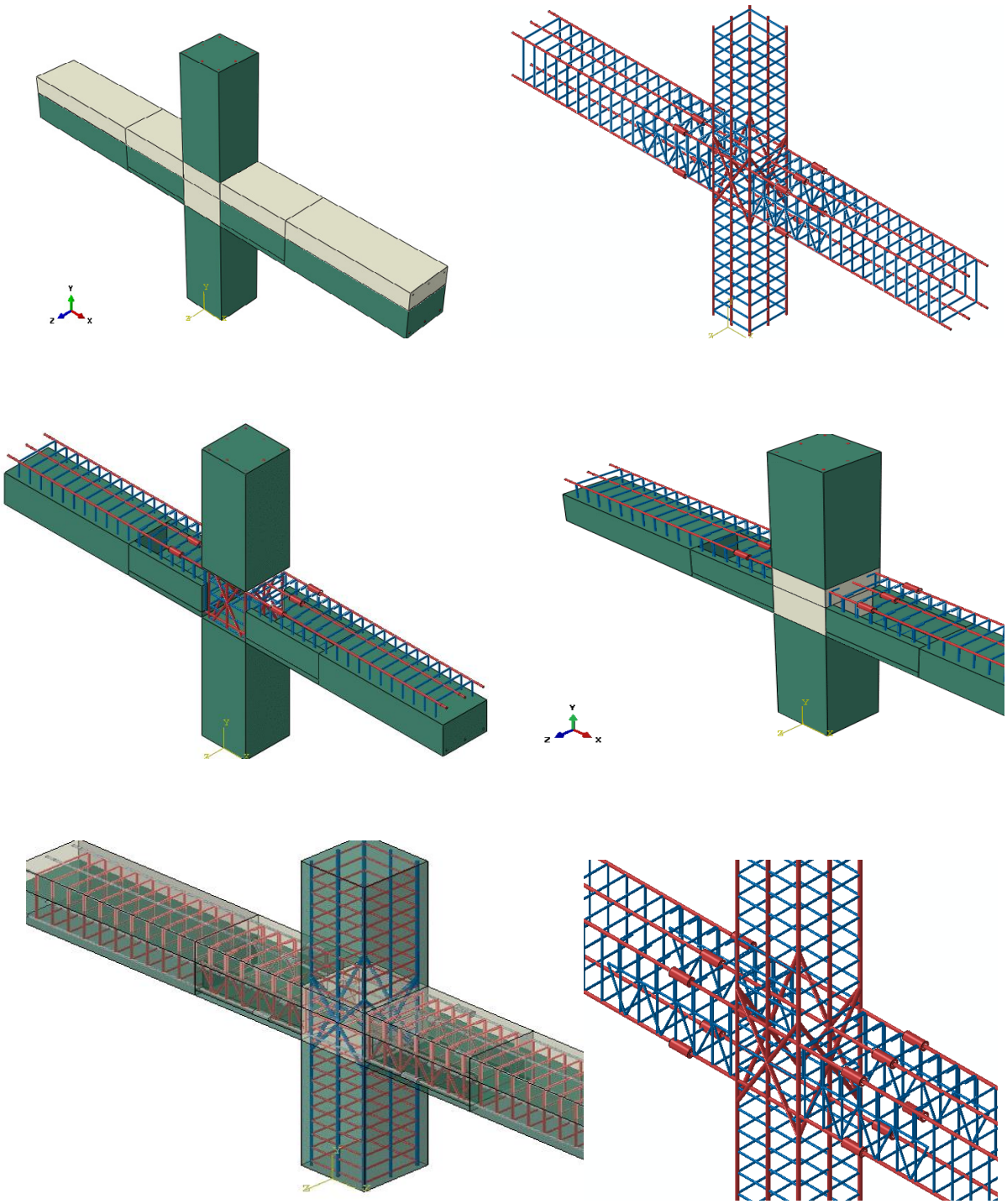

Fig. 10. The 3D model of PCF-1

in monolithic specimen, it created on 50 mm distance from the face of column. Because of existence the grout concrete materials and MRCs couplers in connection area of embedded beams, the development of flexural cracks were gradually moved to 300 mm away from the column face. So in monolithic sample, the more cracks were observed on the 150 mm space uniformly in beam length. By increasing the load magnitude, the new cracking emergence was decreased and the existed cracks were widening progressively in precast specimen. The diagonal shear cracks at core connection were initiated at 3.5% drift for precast specimens so for monolithic specimen was 2.5% drift. According to test observations, the crack's width in failure point reached to about 5mm in face of column for precast specimens and about 1.5mm in monolithic specimen. At the ultimate load cycles, the flexural cracks were appeared at the ends of the precast beams. The compressive strength of the grout caused to a little difference at the initial stage. However, the overall cracking procedure

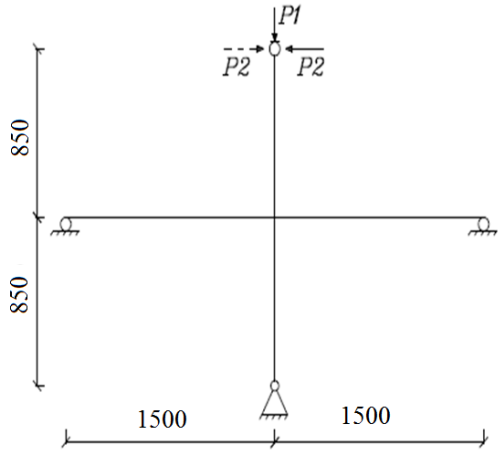

Fig.11. Type of loading and boundary conditions (dimensions are in mm).

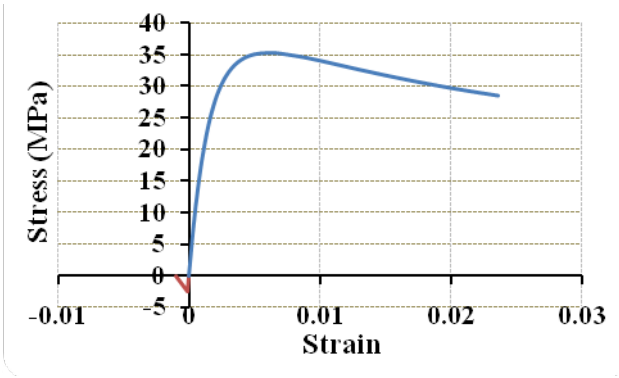

Fig. 12. The stress-strain curve of the confined concrete [19]

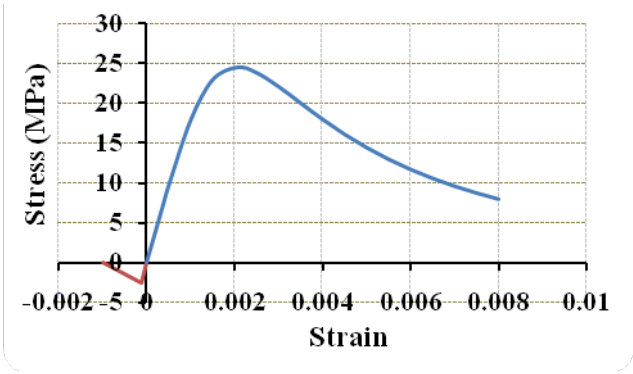

Fig. 13. The stress-strain curve of the unconfined concrete [19]

Table. 3. Plasticity parameters of CDP [18]

ψ	Eccentricity	f	k	Viscosity parameter
31	0.1	1.16	0.667	0.001

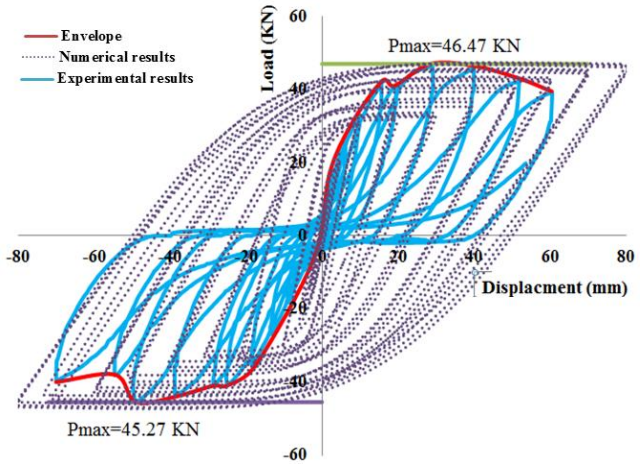

PCC1-Hysteresis

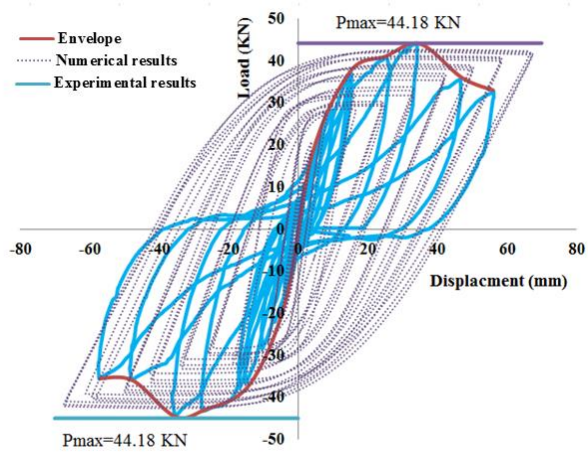

PCF1-Hysteresis

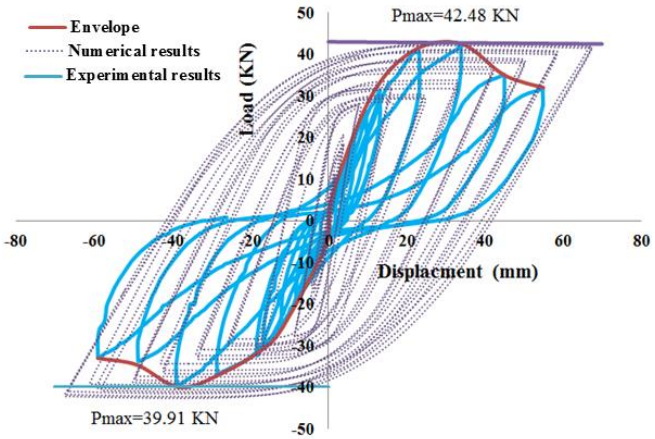

Fig.14. Hysteretic and envelope curves for connections

was not affected by this parameter. Although, the numerical simulation were also predict similar crack propagation pattern but the diagonal shear cracks were triggered with a little delay in comparison to the test results. There is about 9 percent deviation in the crack initiation drift.

Eventually, the flexural cracks govern the final failure of the connection core. The couplers improved the stiffness and strength of the cast in place parts of the connection zone. Since the column strength was higher than the beam in all of

MC1-Experiment photo | PCC1-Experiment photo

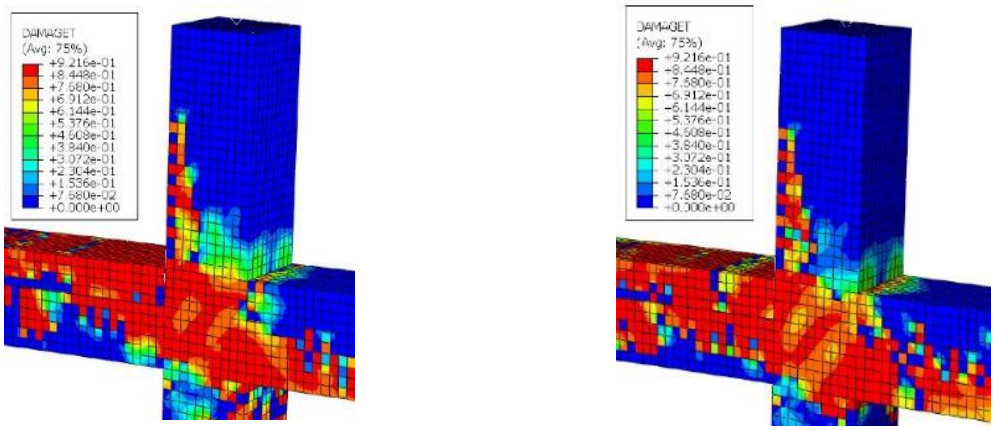

MC1-Tensile damage | PCC1-Tensile damage

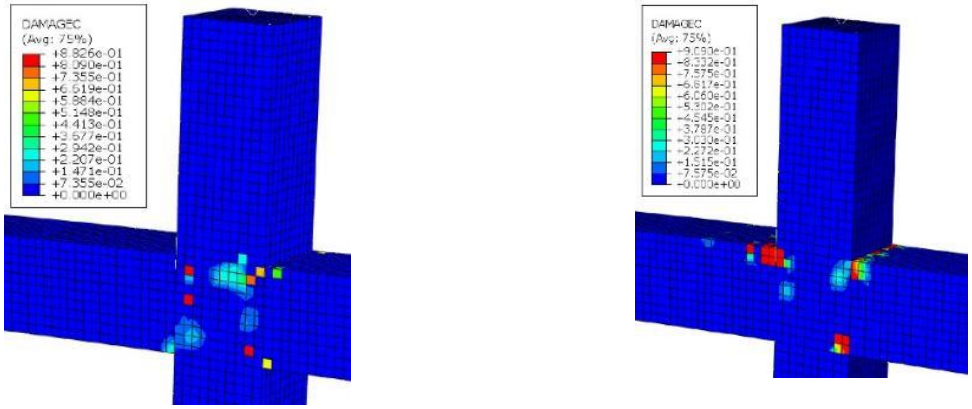

MC1-Compressive damage | PCC1-Compressive damage

Fig. 15. The crack pattern and failure mode of MC1 (monolithic specimen) and PCC1 (precast specimen)

the specimens, the cracks moved from beams to joints then extending to the column.

6-2-Ductility

In table 4, the yield displacements, ultimate ductility (m), story drift at failure and performance level are given. The ability of the structure to endure the permanent deformations without serious deterioration is called ductility. Ductility plays a significant role in the energy dissipations. The ultimate displacement ductility of the connections is expressed as ratio of the ultimate deformation in each cycle to yield deformation. ASCE/SEI standard 41-13 provisions [21] were used to calculate the yield deformation by simulating the envelop hysteresis curve of lateral load-displacement to bilinear curve. Also, the story drift is the relative displacement of column at failure, which is the ratio of ultimate lateral displacement of

Table 4.Evaluation of the ASCE performance level

Specimen	Maximum bending moment (kN.m)	Yield displacement dy(mm)	Ultimate ductility m	Story drift at failure (%)	Performance level
PCC1	46.47	18.09	3.82	4.06	CP
PCF1	44.17	13.11	3.74	3.31	LS
MC1	42.47	14.08	3.11	2.57	LS

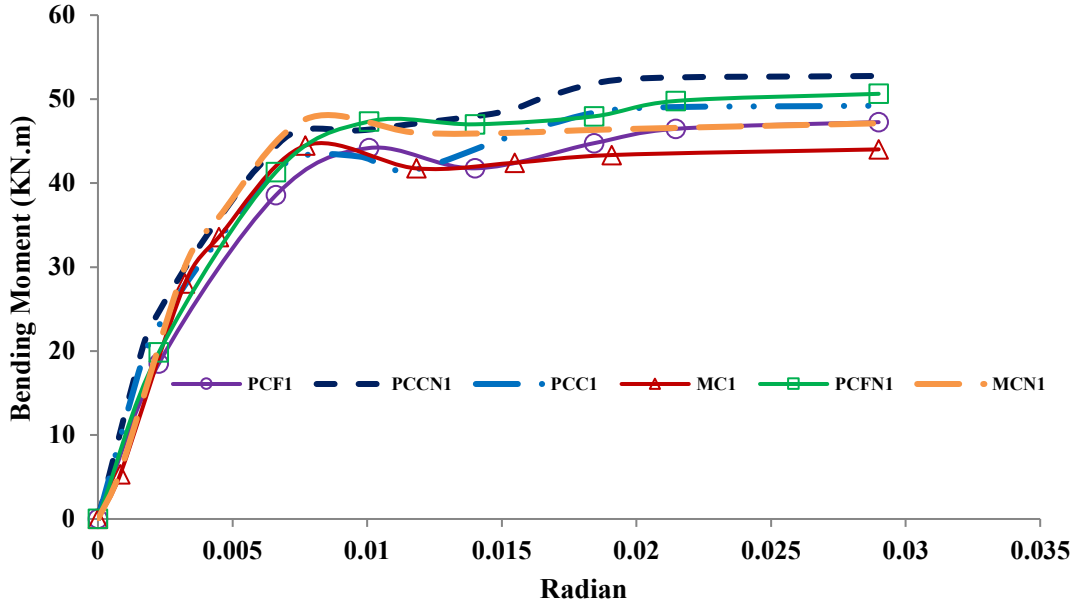

Fig. 16. Moment-rotation envelopes for monolithic and proposed precast connections

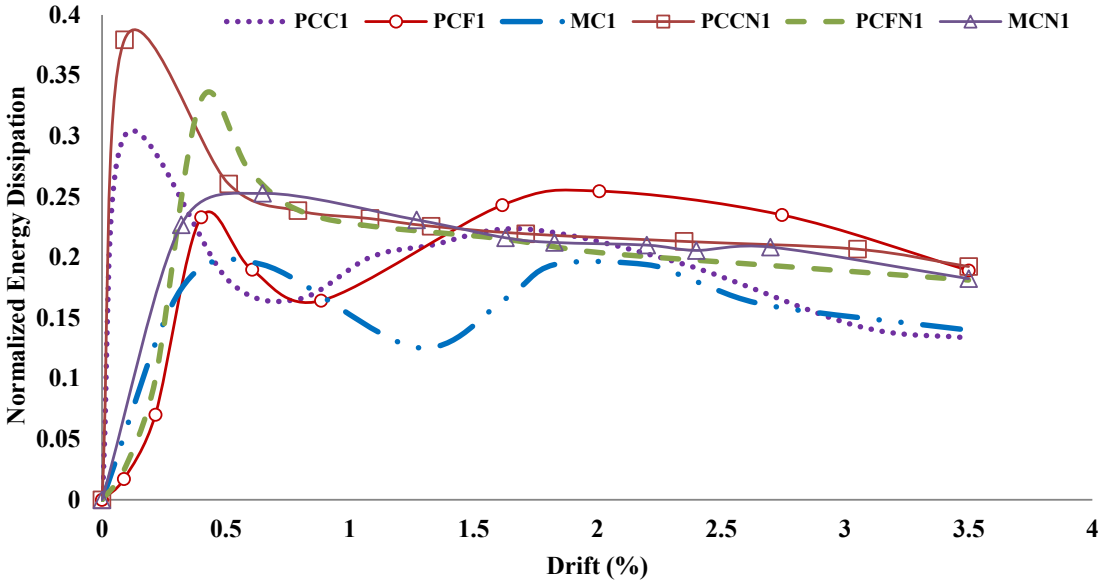

Fig. 17. Normalized energy dissipation

column at failure point to the column length (1750mm). The ductility of precast specimens is more than monolithic one.

6-3-Moment-rotation curves

Moment-rotation curve is drawn to evaluate the flexural rigidity of precast specimens in compare to monolithic specimen (See Fig.. 16). The joint rotation is calculated based on the recorded strains for the top and bottom of the longitudinal bars. Also, bending moments are resulted by multiple the lateral loads to half of column net height. As the first cracks appeared in the connection edges the rotation results passed the linear zone at 0.0075 radians. The moment-

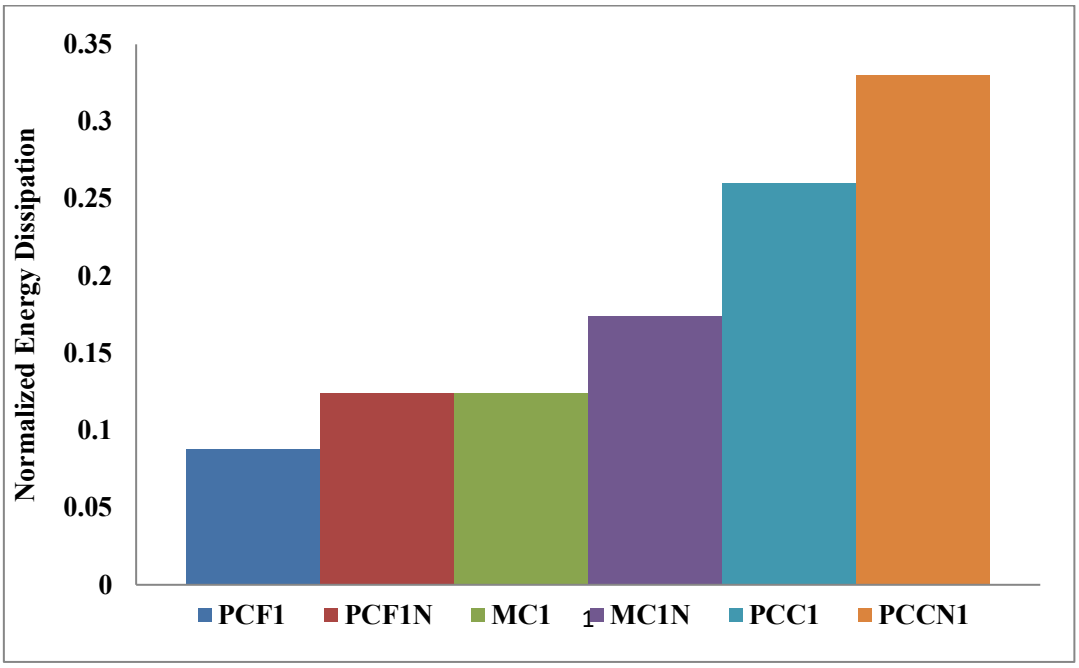

Fig. 18. Normalized energy dissipation at 0.25% drift

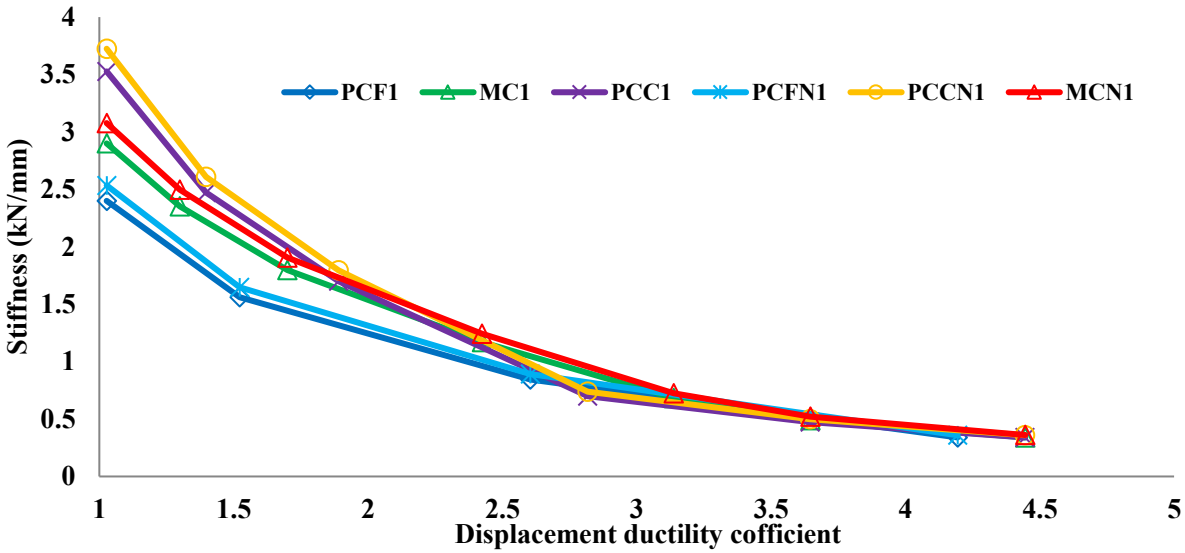

Fig. 19.Connection stiffness degradation

rotation curve experienced a depression around the 0.015 radian due to conversion of the shear cracks in the connection zone to flexural cracks in beams. The variation of results is disappeared by approaching to 0.03 radians of rotation and no moment resistance increase is observed after 0.015 radians. The deviation of the numerical results in comparison with test results is about 7.23 percent. The results of the numerical models are presented with PCCN1, PCFN1, and MCN1 in Fig. 16.

6-4-Energy dissipation

The literature review clarify that there is a very strong relationship between ductility and the energy dissipation capacity of a connection zone. Normalized energy dissipation (NED) is selected to study the coupler arrangement effects. Detailed calculations of NED can be found in ref[8]. The most apparent increase is about 30% and belongs to PCC 1 occurred at 0.25 % drift. The closer coupler in the connection arrangement leads to more amplification of the difference between the results of energy dissipation in relation to the monolithic results (See Fig.17). In the coupler arrangement closer to plastic hinge zone the dissipated energy and the ductility of the specimen are reduced. The deviation of the numerical results in comparison with test results is about 15 percent. The main reason of such a high deviation from experimental energy dissipation results is the lack of numerical

models in simulation of the pinching effects. The results of the numerical models are presented with PCCN1, PCFN1, and MCN1 in Fig.. 17. Fig..18 displays a clustered bar diagram for NED at 0.25 % drift for perceiving the differences better.

6-5- Joint stiffness

Since the joint stiffness was decreased during earthquake, therefore; drawing the stiffness-displacement ductility curve is so important factor in seismic behavior of connection. Fig.19 demonstrates that the stiffness of the beam- column joint reduction by increasing the ductility coefficient. The calculation of joint stiffness was done according to details of ref. [8]. The connection stiffness [8] is so dependent on the coupler array. The specimen PCC1 shows connection stiffness 20 % higher than the monolithic case. The closer couplers to column face leads to more connection stiffness. The results of the numerical models are presented with PCCN1, PCFN1, and MCN1 in Fig. 19.

7- CONCLUSIONS

An experimental study on a proposed moment resisting semi-dry connection of precast frame member was performed under cyclic loading. Two precast half scaled and one monolithic beam-column connection was tested under cyclic lateral load. The main novelty of new connection is application of the mechanical reinforcement couplers, MRCs in precast members. The experiments were conducted to achieve the effect of the different couplers arrangement in the vicinity of the connection zone. A numerical study were carried out parallel to the test program to percept the seismic behavior aspects of the precast connection zone. The following conclusion can be derived according to the test results:

1- The coupler arrangement has no significant effect on the moment capacity of the specimen, but the specimen with the couplers distant 200 mm to column face (PCF1) clearly shows higher flexural strength particularly after 0.015 radian of connection core rotation.

2- The observed crack patterns for precast specimens focused on edge of column while the uniform distributed cracks were created for monolithic connection.

3- The proposed precast connection arrangement reduces the probability of occurrence of undesirable shear failure modes by adding diagonal reinforcement bars in the joint core.

4- According to the laboratory observations, as the wider crack widths are appeared around the connection zone, the dissipated energy goes up more specifically. The maximum energy dissipated by the model PCC1 is about 30 percent more than the monolithic model.

5- The numerical simulation is capable to predict the overall behavior of the precast connection zone. The maximum deviation of the numerical results belongs to the energy dissipation variations due to the pinching effects in the test results. The ultimate values of bearing capacity and displacement show a fair agreement with the experimental results.

6- According to laboratory observation, the proposed precast connection should be constructed by the couplers closer to the column face.

ACKNOWLEDGMENTS

The authors wish to acknowledge the structural laboratory officials of the Science and Culture University gratefully for their supports to conduct experimental program.

REFERENCES

[1] A.-A.C. 550, Guide to Emulating Cast-in-place Detailing for Seismic Design of Precast Concrete Structures, in, American Concrete Institute, 2009.

[2] M.N. Priestley, Overview of PRESSS research program, PCI journal, 36(4) (1991) 50-57.

[3] D. Bull, Guidelines for the use of structural precast concrete in buildings, Centre for Advanced Engineering, University of Canterbury, 2000.

[4] Y. Masuda, M. Iizuka, Revision of "JASS 10 Precast Reinforced Concrete Work", Concrete Journal, 51(4) (2013).

[5] R. Vidjeapriya, K. Jaya, Experimental study on two simple mechanical precast beam-column connections under reverse cyclic loading, Journal of Performance of Constructed Facilities, 27(4) (2013) 402-414.

[6] D. Ejima, Seismic experimental study on a precast concrete beam-column connection with grout sleeves, Engineering Structures, 155 (2018) 330-344.

[7] T. Ozturan, S. Ozden, O. Ertas, Ductile connections in precast concrete moment resisting frames, concrete construction, 9 (2006) 11.

[8] H. Parastesh, I. Hajirasouliha, R. Ramezani, A new ductile moment-resisting connection for precast concrete frames in seismic regions: an experimental investigation, Engineering Structures, 70 (2014) 144-157.

[9] C.-x. Wu, Y. Zhou, W.-s. Lai, Y.-f. Zhang, X.-s. Deng, Experiment on seismic performance of cast-in-situ and prefabricated concrete frame structure joints, J. Archit. Civil. Eng, 32(3) (2015) 60-66.

[10] A. Bai, J. Ingham, R. Hunt, Assessing the seismic performance of reinforcement coupler systems, University of Auckland, 2003

[11] Z.B. Haber, Precast column-footing connections for accelerated bridge construction in seismic zones, University of Nevada, Reno, 2013.

[12] D. Bompa, A. Elghazouli, Inelastic cyclic behaviour of RC members incorporating threaded reinforcement couplers, Engineering Structures, 180 (2019) 468-483.

[13] S. Bahrami, M. Madhkhan, F. Shirmohammadi, N. Nazemi, Behavior of two new moment resisting precast beam to column connections subjected to lateral loading, Engineering Structures, 132 (2017) 808-821.

[14] M. Fathi, M. Parvizi, J. Karimi, M.H. Afreidoun, Experimental and numerical study of a proposed moment-resisting connection for precast concrete frames, Scientia Iranica, 25(4) (2018) 1977-1986.

[15] I.C. Council, B. Officials, C.A. International, I.C.o.B. Officials, S.B.C.C. International, International building code 2009, Cengage Learning, 2009.

[16] ASCE, Minimum design loads for buildings and other structures, in, American Society of Civil Engineers, 2013.

[17] Committee, Building code requirements for structural concrete (ACI 318-05) and commentary (ACI 318R-05), in, American Concrete Institute, 2005.

[18] D. Systèmes, ABAQUS/Analysis User's Guide, Version 2016, Waltham, Massachusetts: Dassault, (2016).

[19] J.B. Mander, M.J. Priestley, R. Park, Theoretical stress-strain model for confined concrete, Journal of structural engineering, 114(8) (1988) 1804-1826.

[20] M. Sargin, Stress-Strain relationships for concrete and analysis of structural concrete sections, Study No. 4, Solid Mechanics Division, University of Waterloo, Waterloo, Ontario, Canada, (1971).

[21] ASCE, Seismic evaluation and retrofit of existing buildings, in, American Society of Civil Engineers, 2014.

[22] M.A. Ab-Kadir, J. Zhang, N. Mashros, A. Hassan, N. Mohd, Experimental and Numerical Study on Softening and Pinching Effects of Reinforced Concrete Frame, IOSR Journal of Engineering, 4(1) (2014).

HOW TO CITE THIS ARTICLE

E. Mobedi, H. Parastesh, A. Khaloo, Effects of mechanical coupler on cyclic behavior of wet connection in precast concrete Frame, AUT J. Civil Eng., 4(1) (2020) 3-16.

DOI: 10.22060/ajce.2019.15680.5547